Earth and Planetary Science Letters 317–318 (2012) 363–373

Contents lists available at SciVerse ScienceDirect

Earth and Planetary Science Letters

journal homepage: www.elsevier.com/locate/epsl

Magnitude and consequences of volatile release from the Siberian Traps

Benjamin A. Black [a,*], Linda T. Elkins-Tanton [a,b], Michael C. Rowe [c], Ingrid Ukstins Peate [d]

[a] Department of Earth, Atmospheric, and Planetary Sciences, Massachusetts Institute of Technology, Cambridge, MA, USA
[b] Department of Terrestrial Magnetism, Carnegie Institution for Science, Washington, D.C., USA
[c] School of Earth and Environmental Sciences, Washington State University, Pullman, WA, USA
[d] Department of Geoscience, University of Iowa, Iowa City, IA, USA

ARTICLE INFO

Article history:
Received 12 March 2011
Received in revised form 23 November 2011
Accepted 1 December 2011
Available online xxxx

Editor: G. Henderson

Keywords:
Siberian Traps
large igneous provinces
mass extinction
end-Permian

ABSTRACT

The eruption of the Siberian Traps flood basalts has been invoked as a trigger for the catastrophic end-Permian mass extinction. Quantitative constraints on volatile degassing are critical to understanding the environmental consequences of volcanism. We measured sulfur, chlorine, and fluorine in melt inclusions from the Siberian Traps and found that concentrations of these volatiles in some magmas were anomalously high compared to other continental flood basalts. For the ten samples for which we present data, volatile concentrations in individual melt inclusions range from less than the detection limit to 0.51 wt.% S, 0.94 wt.% Cl, and 1.95 wt.% F. Degassing from the Siberian Traps released approximately ~6300–7800 Gt S, ~3400–8700 Gt Cl, and ~7100–13,600 Gt F. These large volatile loads, if injected into the stratosphere, may have contributed to a drastic deterioration in global environmental conditions during the end-Permian.

1. Introduction

Almost two decades have passed since the eruption of the Siberian Traps was first proposed as a trigger for the end-Permian mass extinction (Campbell et al., 1992; Renne and Basu, 1991), the largest loss of floral and faunal diversity in Earth's history (Erwin, 1994; Sepkoski et al., 1981). The Permian–Triassic boundary was preceded by an ~1.5 Myr episode of ocean euxinia (Cao et al., 2009) and followed by ~5 Myr of suppressed biological diversity and large fluctuations in the $\delta^{13}C$ record (Lehrmann et al., 2006; Payne et al., 2004). Degassing and atmospheric loading of volatiles is one of the critical mechanisms that links mafic volcanic eruptions with global environmental change (Devine et al., 1984; Thordarson et al., 1996). We seek to quantify volatile flux throughout the evolution of the Siberian Traps large igneous province and to evaluate the potential climatic impact.

The Siberian Traps magmas were erupted through the Tunguska sedimentary sequence, which reaches 12.5 km in thickness (Meyerhoff, 1980). The thickness of Cambrian evaporitic sequences alone can exceed 2.5 km (Fig. 1); Zharkov (1984) estimates that the East Siberian Basin hosts a total volume of ~585,000 km^3 of rock salt. Additional Siberian salt deposits are found in Ordovician through Carboniferous strata (Zharkov, 1984).

Evidence from trace elements (Lightfoot et al., 1990; Wooden et al., 1993), $\delta^{34}S$ (Li et al., 2009b; Ripley et al., 2003), ε_{Nd} (Arndt and Christensen, 1992), magmatic sulfides (Li et al., 2009a), and drill cores through pipe structures (Svensen et al., 2009) provides strong support for widespread interaction between crustal rocks (including evaporites and carbonates) and magmas. Contact heating and metamorphism related to sill intrusion may have led to direct, potentially explosive gas release from the Tunguska sediments (Svensen et al., 2009). In addition to this direct degassing, we suggest that Siberian Traps magmas may have extensively assimilated these volatile-rich sedimentary rocks, increasing their concentrations of dissolved volatiles.

Outcrops of the Siberian Traps stretch from the Taimyr Peninsula in the north of Russia as far south as Bratsk (Fig. 1). With an estimated volume of ~4×10^6 km^3 (Fedorenko et al., 2000), the Siberian large igneous province ranks among the largest known continental flood basalts. Volumetrically, it is roughly three times as large as the Deccan Traps (Jay and Widdowson, 2008), and twenty times as large as the Columbia River Flood Basalts (Coffin and Eldholm, 1994). Although mafic lava flows are most abundant, volcaniclastic and intrusive units also account for large fractions of the total volume. The maximum cumulative thickness of the dolerite sills, which most frequently intrude the Paleozoic sedimentary rocks, has been estimated as 1200 m (Kontorovich et al., 1997).

The precise temporal relationship between the onset of eruption and the main pulse of extinction remains unclear, despite geochronological advances (Bowring et al., 1998; Kamo et al., 2003). Zircon-bearing rocks are rare at the base of all exposed Traps sections,

* Corresponding author.
E-mail addresses: bablack@mit.edu, ben.black@gmail.com (B.A. Black), ltelkins@dtm.ciw.edu (L.T. Elkins-Tanton), mcrowe@wsu.edu (M.C. Rowe), Ingrid-Peate@uiowa.edu (I.U. Peate).

0012-821X/$ – see front matter © 2011 Elsevier B.V. All rights reserved.
doi:10.1016/j.epsl.2011.12.001

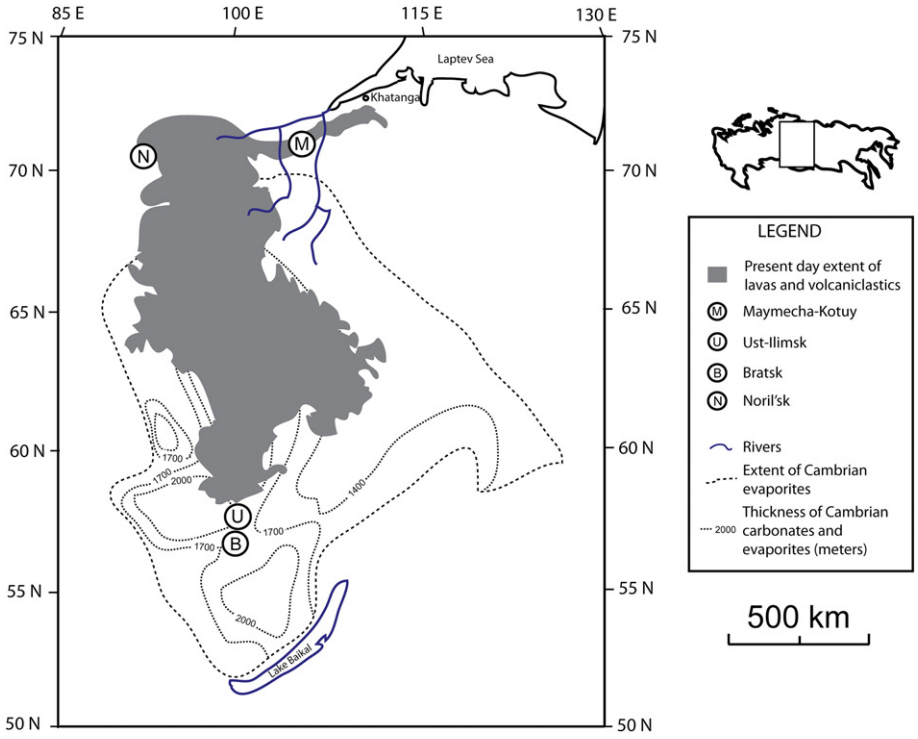

Fig. 1. Map showing present day extent of Siberian Traps lavas and volcaniclastics in the Tunguska basin based on Reichow et al. (2005). Thickness and extent of Cambrian evaporites, including limestone, halite, dolomite and anhydrite, are based on Zharkov (1984). As described in the legend, circled letters M, U, and B denote the three areas from which we obtained melt inclusion samples. N marks Noril'sk, the source of the inclusions reported in Sobolev et al. (2009). Reichow et al. (2005) have also argued that the distribution of intrusions and basaltic subcrop supports a much larger original extent of the Siberian Traps, reaching into the adjacent West Siberian Basin (not shown here).

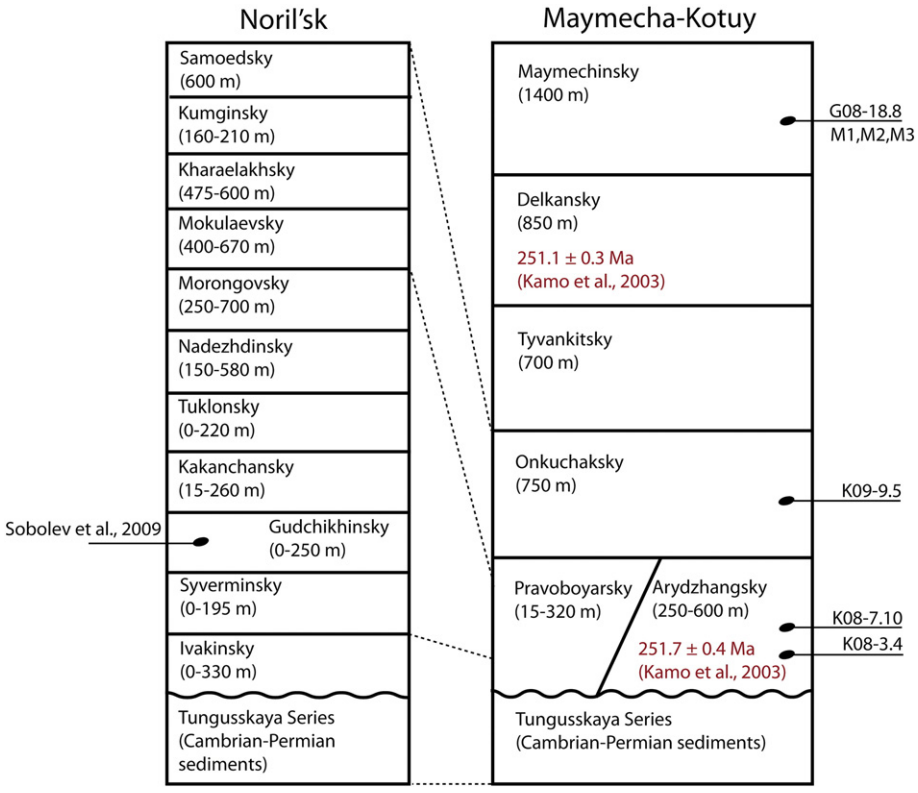

Fig. 2. Schematic stratigraphy of the extrusive suites in the Noril'sk and Maymecha–Kotuy regions of the Siberian Traps, marked with an N and M respectively in Fig. 1. U–Pb dates from Kamo et al. (2003) are given in red; stratigraphic positions of the samples from the Maymecha–Kotuy presented in this study are denoted on the right. The inclusions reported in Sobolev et al. (2009) come from the Gudchikhinsky picrites, as denoted on the left. Dotted lines show geochemical, paleomagnetic, and paleontological correlations between Noril'sk and Maymecha–Kotuy as proposed by Fedorenko and Czamanske (1997), Fedorenko et al. (2000), Kamo et al. (2003). (For interpretation of the references to color in this figure legend, the reader is referred to the web version of this article.)

making ultra high-precision dating of these flows and pyroclastic deposits difficult. U–Pb dating of perovskites in a stratigraphically early Arydzhangsky flow and zircons from a late Delkansky silicic tuff (Fig. 2) suggests that in the Maymecha–Kotuy region the bulk of the eruption occurred in <1 Myr, with onset prior to 251.7 ± 0.4 Ma (Kamo et al., 2003).

Ar–Ar geochronology on plagioclase and biotite has also been used to evaluate the timing of the eruption and the extinction (Renne et al., 1995). However, it is difficult to directly compare Ar–Ar dates with U–Pb dates because of, among other factors, uncertainty in the absolute age of the fluence monitor used during Ar–Ar sample irradiation. Reichow et al. (2009) obtained an Ar–Ar date of 250.3 ± 1.1 Ma for the final stages of extrusive volcanism at Noril'sk, within error of their high precision sanidine Ar–Ar date for the main pulse of the extinction at 249.25 ± 0.14 Ma. Because these dates were produced in the same lab using the same fluence monitor age, they should be directly comparable, suggesting that within uncertainty the eruption overlaps with the main pulse of the extinction.

2. The end-Permian mass extinction

The end-Permian mass extinction was a period characterized by sudden loss of >90% of marine species and >70% of terrestrial species; even insect diversity suffered (Erwin, 1994). Unlike the Cretaceous–Tertiary extinction, which was most likely triggered by the bolide impact that formed the Chicxulub impact crater, no major impact event has been generally accepted as the cause of the end-Permian mass extinction (Farley et al., 2005).

Fossil size and diversity did not begin to recover until ~5 Myr after the beginning of the extinction (Lehrmann et al., 2006; Payne et al., 2004), suggesting that environmental conditions could have been inhospitable for a prolonged period. This paleontological observation is matched by an extended period of large amplitude (up to 8‰) carbon isotope fluctuations following the first pulse of the extinction (Payne et al., 2004). The observed carbon isotopic instability could result either from perturbations in organic carbon burial associated with a damaged ecosystem, or directly from the environmental disturbances driving the extinction (Payne and Kump, 2007; Payne et al., 2004). Carbon cycle modeling suggests that episodic fluxes of magmatic and organic carbon could produce the late Permian and early Triassic carbon isotopic pattern (Payne and Kump, 2007). However, given the size of the oceanic and atmospheric carbon reservoirs and the probable timescale of eruption, the direct climatic warming due to magmatic CO_2 emissions alone was most likely small (Caldeira and Rampino, 1990).

End-Permian and early Triassic deep-sea cherts are preserved in accretionary sections in Japan and British Columbia, and contain pyrite and lack hematite, implying that anoxic conditions prevailed at the time of deposition (Isozaki, 1997). Huey and Ward (2005) cite these anoxic markers and high background extinction rates in the late Permian as evidence that environmental conditions had deteriorated well before the main pulse of the extinction, suggesting that the Permian–Triassic transition occurred in the midst of an extended period of ecological stress.

A kill mechanism is the actual environmental condition that leads to death of an organism, and a trigger mechanism is a perturbation that initiates reactions that lead to that environmental condition (Knoll et al., 2007). Many kill mechanisms have been proposed for the end-Permian mass extinction, including: ocean anoxia, euxinia, and/or sulfide release driven by global warming and decreased ocean circulation (Kump et al., 2005), ozone depletion and mutagenesis (Beerling et al., 2007; Visscher et al., 2004), and elevated carbon dioxide levels (Knoll et al., 2007). Heavily calcified organisms were much more vulnerable to extinction during the end-Permian (Knoll et al., 2007). This suggests that high carbon dioxide levels, also known as hypercapnia, played a significant role in the marine extinction. The Siberian Traps have often been invoked (e.g. Campbell et al., 1992; Payne and Kump, 2007; Svensen et al., 2009) as a trigger mechanism for one or more of the kill mechanisms mentioned above. In particular, the Siberian Traps might have triggered environmental change as a result of degassing related to contact metamorphism of Tunguska sedimentary rocks (Ganino and Arndt, 2009; Kontorovich et al., 1997; Svensen et al., 2009) or as a result of degassing from the magma upon eruption. For example, volcanic sulfur forms sulfate aerosol particles, which can generate global cooling with an e-folding decay time in the atmosphere of ~1 year after the end of the eruption (Barnes and Hofmann, 1997). Cl and other halogens can contribute to ozone destruction in the stratosphere (Beerling et al., 2007; Johnston, 1980; Molina, 1996); sulfate aerosols can provide surfaces for these reactions to proceed (Robock, 2000; Textor et al., 2003).

We investigate the concentrations of dissolved sulfur, chlorine, and fluorine in Siberian Traps melt inclusions in order to assess which kill mechanisms, if any, might have been triggered by degassing from Siberian Traps magmas.

3. Materials and methods

The micrometer-sized enclaves of trapped magma known as melt inclusions can provide a record of pre-eruptive volatile contents such as S, Cl, F, H_2O, and CO_2 (Anderson, 1974; Devine et al., 1984; Metrich and Wallace, 2008). Before melt inclusions are trapped in crystals, degassing may release volatiles, or crystal fractionation may enrich them in the remaining liquid. After entrapment, volatiles (particularly hydrogen) may diffuse out of or into melt inclusions (Qin et al., 1992). Here we assume that no volatiles diffused from the nominally volatile-free host minerals into inclusions, and any diffusion out would make our measurements minimums. Therefore, these volatile measurements are reasonable minimums for the original concentrations in the magmas. Major elements and compatible trace elements may also be affected by post-entrapment diffusive re-equilibration and Fe-loss (Cottrell et al., 2002; Danyushevsky et al., 2000, 2002). This process strongly depends on diffusivities through the host crystal and partition coefficients between the crystal and melt (Qin et al., 1992). Fe-loss will primarily influence Fe and Mg concentrations in olivine-hosted inclusions, and therefore its effect on incompatible volatile elements is likely to be small (Danyushevsky et al., 2000). Because we are primarily interested in pre-eruptive volatile contents, any re-equilibration of the inclusions prior to eruption does not affect our interpretations.

We analyzed by electron microprobe >150 melt inclusions from the Siberian Traps, and we present results from 70 volatile-bearing inclusions. These inclusions were selected on the basis of oxide totals (from 98 to 101.5 wt.%); statistically significant detection of S, Cl, or F; and absence of visible cracks, large spinel crystals, or quench textures. A large fraction of the inclusions we analyzed in samples K08-3.4 and K08-7.10 contained no detectable S, Cl, or F and were probably breached as a result of the strong cleavage in clinopyroxene. We obtained melt inclusions from ten field samples that include dolerite sills near Bratsk and Ust-Ilimsk, crystalline Onkuchaksky and Maymechinsky lava flows, and mafic Arydzhangsky tuffs that are among the earliest erupted Siberian Traps deposits (Figs. 1–2, Table 1). The basalts in the Maymecha and Kotuy basins include both high-alkali and tholeiitic flows (Arndt et al., 1998). The mafic tuffs and the unusual MgO-rich (>18 wt.%) maymechites belong to the alkaline group; the Onkuchaksky flow is tholeiitic. The Maymecha Kotuy section has been described as a more complete section than Noril'sk (Fedorenko and Czamanske, 1997), which is arguably the most studied region of the flood basalts. While correlation among different areas of the Siberian Traps is difficult, according to the stratigraphy proposed by Fedorenko and Czamanske (1997) and reproduced in Fig. 2 our sample set represents close to the full time-span of Traps emplacement.

Table 1
Maximum and mean measured concentrations of S, Cl, and F from melt inclusions from the Siberian Traps, compared with maximum concentrations from the Deccan Traps (Self et al., 2008), the Columbia River Flood Basalts (Blake et al., 2010; Thordarson and Self, 1996), and Laki (Thordarson et al., 1996). The Bratsk sill is from location B in Fig. 1; the Ust-Ilimsk sill is from location U in Fig. 1; and the Arydzhangsky, Onkuchaksky, and Maymechinsky samples are from the Maymecha–Kotuy, which is location M in Fig. 1. Data from the Gudchikhinsky picrites are from Sobolev et al. (2009).

Sample	Description	Maximum S [Mean S] (wt.%)	Maximum Cl [Mean Cl] (wt.%)	Maximum F [Mean F] (wt.%)
R06-07, A10-23.1	Bratsk dolerite sill	0.13 [0.08]	0.94 [0.33]	0.30 [0.17]
R06-09	Ust-Ilimsk dolerite sill	0.14 [0.09]	0.78 [0.32]	1.95 [0.74]
K08-3.4	Arydzhangsky mafic tuff	0.17 [0.10]	0.03 [0.03]	0.30 [0.19]
K08-7.10	Arydzhangsky mafic tuff	0.16 [0.10]	0.07 [0.05]	0.21 [0.16]
K09-9.5	Onkuchaksky lava flow	0.06 [0.04]	0.01 [0.01]	0.16 [0.09]
G08-18.8, M1, M2, M3	Maymechinsky lava flows	0.51 [0.21]	0.15 [0.05]	0.18 [0.16]
SU50, 4270, KhS51-1 (Sobolev et al., 2009)	Gudchikhinsky picrites	0.061 [0.040]	0.193 [0.042]	–
Deccan Traps	Neral lava flows	0.14 [0.085]	0.09 [0.038]	–
Columbia River Flood Basalts	Wanapum lava flows	0.21 [0.197]	0.035 [0.030]	0.145 [0.131]
Laki	Laki lava flows	0.17 [0.17]	0.035 [0.031]	0.08 [0.065]

Recent paleomagnetic results (Pavlov et al., 2011) support this interpretation; virtual paleomagnetic poles are statistically identical between the two sections, but an additional reversed interval is recorded in the upper part of the Maymecha–Kotuy section.

We handpicked olivine, plagioclase, and clinopyroxene grains from crushed and sieved samples. To counteract the effects of post-entrapment crystallization, we reheated our mineral grains in oxygen-fugacity controlled 1-atm furnaces at the University of Iowa and MIT at conditions at or slightly below the quartz–fayalite–magnetite buffer. We maintained the appropriate oxygen fugacity with a CO_2:H_2 gas mixture. Target heating temperatures were estimated using COMAGMAT (Ariskin et al., 1993). Samples were held at target temperatures for only 10 min in order to reduce potential H diffusion (Hauri, 2002), and were then rapidly quenched resulting in homogeneous glassy inclusions. We mounted and polished individual quenched grains until our melt inclusions were exposed at the surface.

For olivine-hosted melt inclusions, we performed olivine addition and subtraction (e.g. Rowe and Lassiter, 2009) to correct for post-entrapment crystallization and over- or under-heating. For plagioclase, the ratio of mineral-melt partition coefficients for calcium and sodium is sensitive to water content (Sisson and Grove, 1993). For melt inclusions from R06-09, the ratio $K_D^{Ca-Na} = (Ca/Na)_{plagioclase}/(Ca/Na)_{liquid}$ ranges from 0.52 to 0.97, with an average K_D^{Ca-Na} of 0.74. Sisson and Grove (1993) report an experimental $K_D^{Ca-Na} = 0.95$ at 8 kbars in an anhydrous magma; the Ca/Na for plagioclase versus the whole rock composition of R06-09 averages 0.60. Because these values of K_D^{Ca-Na} are all ~1, it is difficult to employ measurements of K_D^{Ca-Na} to detect post-entrapment crystallization and consequent disequilibrium between the host crystal and inclusion. For clinopyroxene-hosted inclusions, equilibrium models for calcium, magnesium, and iron compositions require estimates of pressure and temperature (e.g. Putirka, 1999); as a result, correction on the basis of modeled clinopyroxene-liquid equilibrium might introduce additional uncertainties. Volatiles and other incompatibles not present in the crystal should be minimally affected by any over- or under-heating. The plagioclase- and clinopyroxene-hosted inclusions are therefore presented as measured values, without further correction. However, given the large observed variation in volatile concentrations, this does not significantly affect our results.

Sulfur, chlorine, and fluorine microprobe analyses were performed with the JEOL-JXA-8200 Superprobe at the MIT Microprobe Facility in Cambridge, MA. We employed a 15 kV voltage, and a 10 nA current. The beam diameter was 10 μm for glass analyses and 1 μm for analyses of host crystals. All counting times were 40 s, except for Na and F, which were 5 and 10 s respectively. Nominal detection limits are approximately 0.13 wt.% for F and 0.017 wt.% for S and Cl, although generally consistent repeat measurements for F (Table A.1) suggest that the actual detection limits for F may be lower. Additional S, Cl, F, carbon, and water measurements were performed at the WHOI National SIMS Facility with a Cs- beam on a Cameca 1280 SIMS. Carbon and water analyses are in progress. Initial results show a range of carbon concentrations between ~0.02 wt.% and ~0.33 wt.% C. These maximum C contents, which occur even in samples not carbon-coated prior to ion probe analysis, are higher than we might reasonably expect on the basis of CO_2 solubility (Newman and Lowenstern, 2002). We cannot exclude the possibility that, despite careful sample selection, a minor amount of C-rich exogenic material might have been incorporated into some glasses during the homogenization process.

Electron microprobe and SIMS analyses were calibrated using a combination of natural and synthetic standards. We discarded electron microprobe glass analyses with totals outside the range of 98 to 101.5 wt.%. A complete listing of the whole rock, microprobe and ion probe results for melt inclusions presented here is shown in Supplementary Appendix A, Table A.1.

4. Results: degassing from the Siberian Traps

Our melt inclusions display significant variability in volatile concentrations, and occasionally in major element compositions. Fig. 3

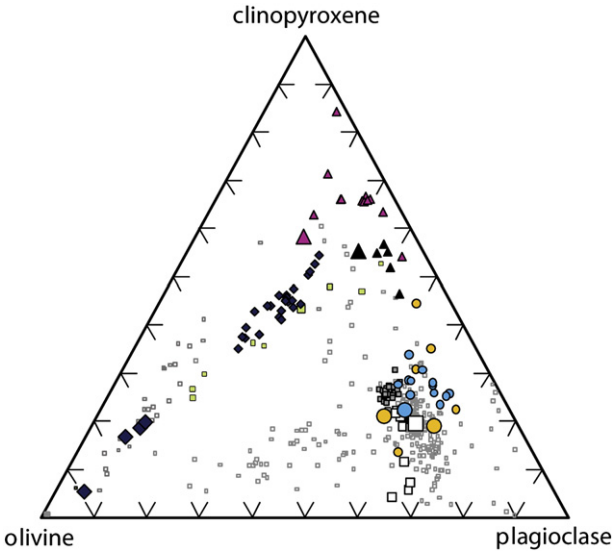

Fig. 3. Modal olivine–clinopyroxene–plagioclase ternary diagram showing whole rock and melt inclusion chemistry compared with previous whole rock and melt inclusion studies of the Siberian Traps. Large colored symbols represent whole rock compositions, and small colored symbols represent melt inclusion compositions: R06-07 and A10-23.1, Bratsk dolerite sill (●); R06-09, Ust-Ilimsk dolerite sill (●); K08-3.4, Arydzhangsky tuff (▲); K08-7.10, Arydzhangsky tuff (▲), G08-18.8, M1, M2, and M3, maymechites (◆), and K09-9.5, Onkuchaksky flow (□). Sobolev et al.'s (1991) maymechite melt inclusion compositions (■) are consistent with our new maymechite inclusions. Sobolev et al.'s (2009) Gudchikhinsky picrite melt inclusions are shown as small gray squares (■). Whole rock geochemical analyses from Arndt et al. (1995), Dalrymple et al. (1995), Fedorenko and Czamanske (1997), Fedorenko et al. (1996), Hawkesworth et al. (1995), Lightfoot et al. (1990), Ryabov et al. (1985), Sharma et al. (1991), Wooden et al. (1993) and Zolotukhin and Almukhamedov (1988) are shown in the background (■).

shows a ternary olivine–clinopyroxene–plagioclase diagram of the whole rock compositions of the ten samples for which we present data. The Siberian Traps are vast and complex, with a surprising variety of magma compositions. Although not all these varieties have been included in this study, the whole rock data in Fig. 3 show that our samples span a large portion of the compositional space occupied by Siberian Traps magmas, as previously reported by Arndt et al. (1995), Dalrymple et al. (1995), Fedorenko and Czamanske (1997), Fedorenko et al. (1996), Hawkesworth et al. (1995), Lightfoot et al. (1990), Ryabov et al. (1985), Sharma et al. (1991), Sobolev et al. (2009), Wooden et al. (1993) and Zolotukhin and Almukhamedov (1988). Our maymechite melt inclusions follow an olivine-control line similar to that of the ten inclusions reported in Sobolev et al. (1991). The olivine-rich whole rock compositions imply that these samples may be olivine cumulates.

Aside from the maymechites, most melt inclusions cluster tightly around their whole rock host compositions, suggesting that those inclusions are representative of their host rocks and that rehomogenization temperatures were close to the temperatures of entrapment. The exceptions are the inclusions from Arydzhangsky tuff K08-3.4 and the Bratsk sill sample R06-07 (Fig. 3, Table A.1). The inclusions in K08-3.4 are significantly more MgO-rich than their host rock and may therefore be samples of a parental magma. The three inclusions in R06-07 are more silicic than their basaltic host rock. They may have experienced post-entrapment crystallization, or they may be sampling a more evolved magma. Regardless, these inclusions have lower Cl and F concentrations than the plagioclase-hosted inclusions from A10-23.1, and consequently our estimates of volatile contents are not significantly skewed by any incompatible fractionation.

For the ten samples for which we present data, volatile concentrations in melt inclusions range from below the detection limit to 0.51 wt.% S, 0.94 wt.% Cl, and 1.95 wt.% F. We present the maximum and mean S, Cl, and F concentrations for each set of samples in Table 1. Maximum concentrations may be more useful than averages or ranges because of the wide spread in values for many samples and because the lowest concentrations may represent partial degassing.

As shown in Table 1, maximum concentrations of S are more consistent than Cl or F across tuff, sill, and lava samples (except the maymechites), with a range between 0.06 wt.% and 0.17 wt.%. Melt inclusions from the high MgO maymechite lavas contain S concentrations up to 0.51 wt.%. Chlorine ranges from 0.01 wt.% in a columnar basalt flow up to 0.94 wt.% in a dolerite sill. Fluorine ranges from 0.16 wt.% in the columnar basalt flow up to 1.95 wt.% in a second dolerite sill. Aside from the sills, Cl ranges from 0.01 wt.% to 0.15 wt.%, and F ranges from 0.16 wt.% to 0.30 wt.%.

In addition to the high sulfur maymechites, some of our melt inclusions are substantially enriched in Cl and F compared to maximum concentrations measured in Deccan Traps, Columbia River Flood Basalts, and Laki melt inclusions (Blake et al., 2010; Self et al., 2008; Thordarson and Self, 1996; Thordarson et al., 1996) (Table 1, Fig. 4). In particular, the two massive sills mentioned above contain high concentrations of Cl and/or F. While it is difficult to precisely constrain sill volumes, where these two sills have outcrops along the Angara River they reach 80–120 m in thickness, and stretch for tens to hundreds of kilometers laterally. Melt inclusions from Noril'sk have also been reported to show moderate enrichments in Cl (Sobolev et al., 2009; Figs. 4 and 5).

On the basis of our own field work and previous mapping and stratigraphic efforts (Fedorenko and Czamanske, 1997; Fedorenko et al., 2000; Malitch et al., 1999), we calculate approximate present-day volumes of individual flows and tuffs from the Maymecha–Kotuy area for which we have melt inclusion data. Because of erosion, these volume estimates probably represent lower bounds. Using the maximum volatile contents of each unit in Table 1, we find that individual flows and tuffs each contained on the order of a combined 10^2 to 10^3 Mt of dissolved S, Cl, and F prior to degassing (Table 2). Estimated eruption times for individual lava flows within the Roza member of the Columbia River Flood Basalts range from 0.3 to 4.5 years

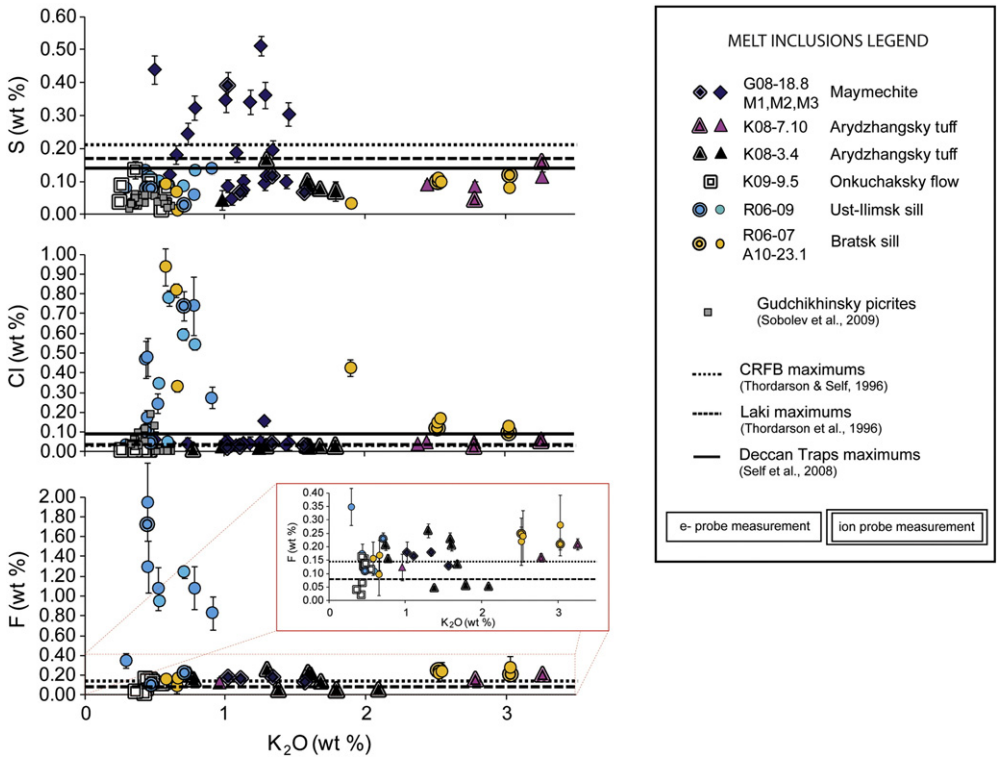

Fig. 4. S, Cl, and F in Siberian Traps melt inclusions. Bottom inset (red box) shows an enlargement of F measurements less than 0.40 wt.%. Error bars are 2-sigma. Where multiple analyses were available for the same target, error bars represent two standard deviations of the population. Otherwise, for microprobe analyses error bars are derived from counting error divided by the square root of the number of measurement points. For SIMS analyses error was calculated on the basis of the goodness of fit to the standard analyses. Double-outlined data points were obtained with ion-probe analysis; ion probe detection limits for Cl are <0.0045 wt.%, and for F are <0.009 wt.%.

Table 2
Dissolved volatiles prior to degassing, based on volumetric estimates and maximum concentrations measured in melt inclusions from each sample (Table 1). Data from the Columbia River Flood Basalts suggests that during the Roza eruption of that large igneous province, approximately 70% of magmatic S, 37% of Cl, and 30% of F were released at the vents (Thordarson and Self, 1996). Volumes are based on present-day thickness and areal extent (Fedorenko and Czamanske, 1997; Fedorenko et al., 2000; Malitch et al., 1999). The range represents the current areal extent of individual suites versus the entire area covered by Maymecha–Kotuy lavas (~16,000 km^2). These volume estimates may incorporate additional uncertainty, given the challenges to mapping in the area and the effects of erosion. Note that the thicknesses of individual flows within the maymechite pile (samples G08-18.8, M1, M2, and M3) are generally difficult to distinguish; the volatile contents of individual Maymechinsky flows in the leftmost columns are therefore omitted.

Extrusive sample	Individual flow/tuff				Suite in Maymecha–Kotuy			
	Volume	S	Cl	F	Volume	S	Cl	F
	(km^3)	(Mt)	(Mt)	(Mt)	(km^3)	(Gt)	(Gt)	(Gt)
K08-7.10	4–112	18–500	8–220	24–660	300–6400	1.4–30	0.4–9	2.1–46
K08-3.4	9–240	42–1100	8–200	76–2000				
K09-9.5	16–128	27–220	4–36	72–570	1500–12,000	2.5–20	0.4–3.3	6.7–54
G08-18.8 M1, M2, M3	–	–	–	–	90–22,400	1.3–320	0.38–94	0.45–110

based on the thickness of lava inflation crusts (Thordarson and Self, 1998). If the style and timing of Siberian volcanism was similar, episodes of magmatism may have delivered highly concentrated pulses of volatiles to the atmosphere. Paleomagnetic secular variation suggests these pulses may have been very compressed—possibly totaling $<10^4$ years (Pavlov et al., 2011). The climate effects of volcanic gases other than CO_2 last ~1–10 years (Timmreck et al., 2010; Wignall, 2001). If periods of quiescence between eruptive events were longer than this, emissions from individual eruptive events may be crucial to understanding environmental consequences. However, the currently available volume and timing constraints are less robust for individual eruptions, as shown by the range in our volume estimates. We therefore focus on an estimate of overall degassing from the Siberian Traps.

Groundmass glass was absent or altered in our samples. In order to estimate degassing behavior for the Siberian Traps, we compared degassing data from the other flood basalt provinces and eruptions for which melt inclusion and groundmass glass measurements have been published (Table 3). Large differences in scale and duration of magmatism exist between the Siberian Traps and Laki, the Deccan Traps, and the Columbia River Flood Basalts (Coffin and Eldholm, 1994; Reichow et al., 2009; Thordarson and Self, 1993). Nonetheless, because of the parallels in the style of these eruptions, the similar S, Cl, and F contents of many of the lavas (e.g. Thordarson and Self, 1996), and the more extensive information about their structure, they provide the best available analogues for the Siberian Traps. The ratio $(Al_2O_3 + CaO + Na_2O + MgO)/SiO_2$ correlates with Cl solubility in basalts (Webster et al., 1999). In Table 3, we calculate this ratio for mean whole rock geochemistry from Laki, the Deccan Traps, and the Columbia River Flood Basalts. The ratio from those three flood basalts is very similar to the ratio from the Siberian Traps, suggesting that they are strong analogs for understanding Cl degassing from our samples.

The degassing efficiencies of S, Cl, and F are relatively consistent for the eruptions presented in Table 3. On average, approximately 64% of magmatic S, 36% Cl, and 30% F were released at vents, and in feeder dikes 44% S, 25% Cl, and 26% F were released (Self et al., 2008; Thordarson and Self, 1996; Thordarson et al., 1996). While degassing efficiencies from feeder dikes–especially feeder dikes involved in phreatomagmatic interactions like the source for these Laki matrix glass samples–are probably substantially different from sills, unfortunately no data are available on degassing of sills related to flood basalt emplacement.

We do not include degassing budgets from non-flood basaltic eruptive centers such as Kilauea, despite the wealth of data, because of the influence that eruptive style and volatile contents may have on degassing efficiencies. It should be noted, however, that Cl and F degassing from Kilauea is significantly lower than what we calculate in Table 3 (Gerlach and Graeber, 1985). Edmonds et al. (2009) find that halogen partition coefficients between fluid and melt are generally low for Kilauea, and that degassing of Cl and F does not begin until shallow depths (~35 m) in the conduit. Halogen degassing behavior is highly dependent on the partition coefficients for Cl and F; Edmonds et al. (2009) rely on glass data from Kilauea, but experimental data on halogen partitioning in basalts are scarce (Carroll and Webster, 1994; Webster et al., 1999). Chloride solubility in molten basalt is approximately 1.25 to 2.9 wt.% (Carroll and Webster, 1994; Webster et al., 1999). As Cl concentrations approach these solubilities, $D_{Cl}^{vapor/melt}$ increases (Webster et al., 1999). Thus for Siberian sills with high Cl, degassing of Cl may be more favorable than at volcanoes like Kilauea, where magmatic Cl concentrations are <0.035 wt.% (Hauri, 2002). Cl solubility also decreases with increasing silica content in the melt, such that crystallization in the sills could lead to a Cl-driven 'second boiling' (Webster et al., 1999), which would allow degassing of a Cl-rich vapor after sill emplacement.

The total volume of the Siberian Traps was roughly $\sim 4 \times 10^6$ km^3 (Fedorenko et al., 2000). Excluding anomalously high S concentrations in the maymechites, we average the maximum and mean concentrations (Table 1) observed in each of our extrusive samples along with the Gudchikhinsky picrites reported in Sobolev et al. (2009) to obtain an estimate of typical volatile contents. Maximum concentrations yield estimates of 0.11 wt.% S, 0.09 wt.% Cl, and

Table 3
Degassing of S, Cl, F, and H_2O, where data is available, from lavas and feeder dikes in flood basaltic eruptions. Estimates of degassing from Laki are from Thordarson et al. (1996), and the ranges represent vent degassing vs. total degassing; feeder dike estimates are based on comparison of melt inclusions with volatiles in groundmass glass from phreatomagmatic tephra clasts. Estimates from the Deccan Traps are from Self et al. (2008), and the ranges represent crystallinity-corrected versus measured results. Estimates from the Columbia River Flood Basalts are from Thordarson and Self (1996) and the ranges represent vent degassing versus total degassing. The ratio $(Al_2O_3 + CaO + Na_2O + MgO)/SiO_2$ correlates with Cl solubility in basalts (Webster et al., 1999), and was calculated based on whole rock geochemistry from the studies mentioned above. In the case of the Siberian Traps, the ratio was calculated based on mean whole rock major elements for the samples used in this study, which are shown in Table A.1.

Eruption	$\frac{Al_2O_3 + CaO + Na_2O + MgO}{SiO_2}$	S		Cl		F		H_2O
		(% degassed)		(% degassed)		(% degassed)		(% degassed)
		Lava	Feeder dikes	Lava	Feeder dikes	Lava	Feeder dikes	Lava
Laki	0.65	71–88	44	27–51	33	29–52	37	70–90
Deccan Traps	0.69	50–74	N/A	44–72	N/A	N/A	N/A	N/A
Columbia River Flood Basalts	0.58	70–90	44	37–66	17	30–37	15	N/A
Mean	0.64	64–84	44	36–63	25	30–45	26	70–90

0.21 wt.% F in the extrusive rocks; mean concentrations from each sample yield estimates of 0.10 wt.% S, 0.04 wt.% Cl, and 0.15 wt.% F. Assuming a total extrusive volume of $\sim 3\times10^6$ km^3 and the vent degassing percentages from Table 3, the Siberian Traps tuffs and lavas may conservatively have released ~5300–6100 Gt S, ~1100–2700 Gt Cl, and ~3800–5400 Gt F.

On the basis of our three sill samples (from two sills), we can extrapolate to a rough estimate of degassing potential from $\sim 1\times10^6$ km^3 of intrusives (personal communication, M. Reichow; Vasil'ev et al., 2000). Assuming degassing efficiencies similar to feeder dikes from Table 3, ~1000–1700 Gt S, ~2300–6000 Gt Cl, and ~3300–8200 Gt F could have degassed from intrusive rocks.

The sum of degassing from intrusive and extrusive rocks leads to total magmatic degassing estimates from the Siberian Traps of approximately ~6300–7800 Gt S, ~3400–8700 Gt Cl, and ~7100–13,600 Gt F. The range in these estimates represents the difference between averaging mean versus maximum concentrations in melt inclusions from each sample. As mentioned above, intrusion of sills into sedimentary rocks, some of which host petrochemical deposits, has also been proposed as a trigger for gas release related to heating and contact metamorphism of country rock (Svensen et al., 2009). This direct degassing from sedimentary rocks is independent of and would be in addition to our estimates of volatiles degassed from the melts. The presence of immiscible sulfide deposits such as those at Noril'sk (Naldrett et al., 1992) also suggests that the petrologic estimates of the sulfur budget presented here may be minimums.

Our results highlight the importance of sills and other intrusive rocks, which may represent ~25% of the total volume of the Siberian Traps. The contribution of sills to volatile flux is highly dependent on degassing efficiency; based on the initial results presented here, the sills may have hosted a tremendous reservoir of dissolved halogens, including ~9000–24,000 Gt of Cl and ~13,000–32,000 Gt of F. Because they intrude into sedimentary and igneous rocks ranging in age from Proterozoic to Permian (Kontorovich et al., 1997), and because high-precision U–Pb dates are sparse, little is known about the chronology of sill emplacement.

The maymechites are considered the last extrusive products of Siberian Traps magmatism (Fedorenko and Czamanske, 1997). Our maymechite melt inclusions suggest these lavas may have discharged a large pulse of sulfur (Table 3) during the waning stages of Siberian Traps magmatism.

5. Discussion

5.1. Potential sources for magmatic volatiles

The volatile contents we measure in our melt inclusions may derive, to varying degrees, from a combination of mantle melting, assimilation of volatile-bearing crustal materials, and fractionation.

The share of volatiles contributed by mantle melting may have been significant for magmas originating from very low-degree partial melts. On the basis of primitive melt inclusions from the Siqueiros Fracture Zone, average Cl and F contents of the mantle have been estimated as $.0001\pm0.00005$ wt.% Cl, and $.0016\pm0.0003$ wt.% F (Saal et al., 2002). Mid-Ocean Ridge Basalts contain roughly .0002–0.04 wt.% Cl (Michael and Cornell, 1998) and $.025\pm0.005$ wt.% F (Schilling et al., 1980). Recently, Sobolev et al. (2011) have suggested that deep melting of a pyroxenitic source could also contribute to the volatile budget. Arndt et al. (1998) suggest that the alkaline series of Maymecha–Kotuy basalts may result from low-degree melting at great depths (possibly >100 km) in the mantle, whereas the tholeiites may have been extensively processed in shallow crustal magma chambers. Thus the volatile contents of the alkaline tuffs and the maymechites may derive in part from low-degree melting of the mantle.

For the sills and tholeiites, assimilation and fractionation may have played a greater role. Fig. 5 shows the Cl/K_2O ratio plotted against K_2O. Our melt inclusions and those described in Sobolev et al. (2009) demarcate two separate trends, one steep and one shallow. Assuming that the partitioning behavior of Cl is similar to that of K (Kent et al., 1999b), the steep trend is consistent with assimilation of Cl-rich crustal materials such as evaporites, whereas the shallow trend may represent fractionation. In Mid-Ocean Ridge Basalts, a steep Cl/K_2O trend may result from assimilation of seawater-derived hydrothermal minerals or brines (e.g. Kent et al., 1999a; Michael and Schilling, 1989). The dolerite sills and some of the Sobolev et al. (2009) picrites trend to particularly high values of Cl/K_2O. The sills were emplaced in the southern part of the Tunguska basin (Fig. 1), where evaporite, salt, and other sedimentary layers approach maximum thicknesses. The high Cl/K_2O ratios in these rocks provide support for the hypothesis that some intruding magmas assimilated the sedimentary host rocks.

Lightfoot et al. (1990) and Wooden et al. (1993) suggest that crustal contamination may have been greatest early in the volcanic sequence at Noril'sk, peaking in the Nadezhdinsky Suite, with generally decreasing crustal isotopic and trace element signatures toward the later stages of volcanism. Sulfur isotopes at Noril'sk require assimilation of small amounts of country rock; ≤0.5% assimilation of the S-rich evaporites would be sufficient to explain the observed signatures (Ripley et al., 2003). Such assimilation could also affect the oxygen fugacity and thus the solubility of S (Mavrogenes and O'Neill, 1999; Wallace and Carmichael, 1992) and halogen species (Carroll and Webster, 1994; Webster et al., 1999).

5.2. Consequences of degassing for the Permian–Triassic environment

The injection of sulfur, chlorine, and fluorine into the upper atmosphere could have effects ranging from direct toxicity and acid rain to temperature change (Devine et al., 1984) and ozone depletion (Johnston, 1980). The prevalence of mutant pollen tetrads at the time of the end-Permian extinction has been invoked as evidence for ozone destruction, possibly related to volcanic emissions of chlorine and fluorine compounds (Visscher et al., 2004). The implications for chemical weathering processes and ocean chemistry of volcanic degassing on the scale of the Siberian Traps also deserve further study.

Eruption rates are one important and poorly constrained determinant of the environmental impact of the Siberian Traps. The scale of

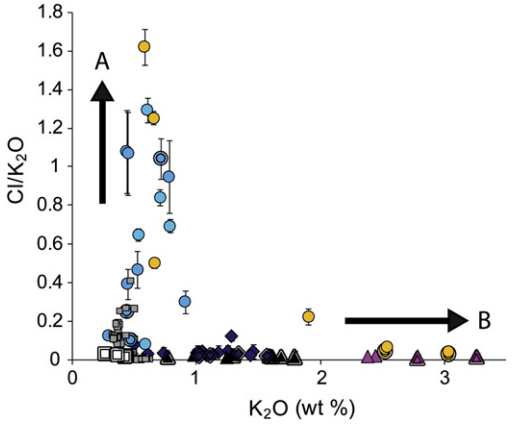

Fig. 5. Cl/K_2O ratios for melt inclusions from the Siberian Traps, including Gudchikhinsky picrites reported by Sobolev et al. (2009). Symbols are identical to those in Figs. 4 and 5. Two trends are visible. Trend A is a near-vertical increase in Cl/K_2O ratios, which may represent assimilation. Trend B may represent other magmatic processes, in particular fractionation. These trends resemble assimilation and fractionation trends observed in Mid-Ocean Ridge Basalts (Saal et al., 2002). In the case of MORB, assimilation of a hydrothermal brines or Cl-rich minerals may lead to Cl/K_2O ratios >0.3 (Kent et al., 1999a; Michael and Schilling, 1989).

climatic repercussions from degassing also depends on several additional key factors, including: (1) Will an ascending thermal plume penetrate the tropopause? (2) What percentage of S, Cl, and F will be delivered to the stratosphere and how long will they remain there? (3) What chemical form will the S, Cl, and F take and what are the probable climatic effects, if any, of the introduction of those species to the upper atmosphere? We investigate these questions further in the following sections.

5.3. Plume heights associated with basaltic eruptions

Delivery to the stratosphere is a critical prerequisite for ozone depletion and global climatic effects. In the Permian, Siberia was located at high latitudes, comparable to its present day position (Cocks and Torsvik, 2007). Because convective mixing is less vigorous at high latitudes, the tropopause occurs at a much lower altitude. The altitude of the tropopause is also seasonally variable, but at 60°N, the transition from the troposphere to the stratosphere occurs at an annual-mean altitude of roughly 10 km (Grise et al., 2010). Several processes might have enabled erupted material to reach the stratosphere, including thermal plumes and phreatomagmatic episodes.

Simple early models suggested that large fissure eruptions such as those often associated with flood basalt provinces might produce thermal plumes that could exceed 10 km in height, thereby reaching the high-latitude stratosphere (Stothers et al., 1986). More recent and realistic modeling shows that vent geometry and eruption rate in particular exercise strong control over plume height (Glaze et al., 2011).

The possibility of relatively long lasting individual flood basalt eruptions, with inflated sheet lobes, implies that typical volumetric eruption rates may be on the order of 10^3–10^4 m^3/s, similar to Laki (Bryan et al., 2010; Keszthelyi et al., 2006; Self et al., 1996). Rubbly, broken-up pahoehoe observed at Laki and the Columbia River Flood Basalts provides evidence for episodes of high-volume eruption that may have reached ~10^6 m^3/s (Keszthelyi et al., 2006). The detection of synchronous Laki-derived sulfates, ash, and trace elements in Greenland ice cores, and witness accounts of eruption columns >9 km high persisting into August 1783, suggest that the Laki plume reached the lower stratosphere (Thordarson and Self, 2003; Wei et al., 2008). If discharge rates and patterns for the Siberian Traps were comparable to those of Laki and the Columbia River Flood Basalts, some of these intermittent periods of rapid effusion may have generated thermal plumes that breached the high-latitude tropopause.

The presence of tuffs, tuff breccias, and volcaniclastic sequences tens to hundreds of meters thick near the base of the volcanic sequence in the Maymecha–Kotuy and Angara regions may reflect explosive episodes that could have enhanced the potential for volatile addition to the stratosphere, due to more rapid eruption rates (Naumov and Ankudimova, 1995). These volcaniclastic rocks account for ~20–30% of the total volume of the Siberian Traps (Ross et al., 2005). They are characterized by poor sorting, sedimentary and volcanic clasts ranging up to ~1 m in diameter, and locally abundant accretionary lapilli that are consistent with a phreatomagmatic origin (Gilbert and Lane, 1994; Schumacher and Schmincke, 1995). The sedimentary clasts suggest that a significant proportion of the explosive activity may have been driven by magmatic interaction with deep aquifers, possibly with additional contributions from surface water. The volcaniclastic rocks will be described in greater detail in a separate paper.

Entrainment of atmospheric water vapor may increase the plume height by several kilometers for small mass eruption rates (10^3–10^6 kg/s), through the additional release of latent heat during condensation (Woods, 1993). Walker et al. (1984) estimate a vent exit velocity of 250–350 m/s in the case of the basaltic plinian Tarawera eruption of 1886, which generated a column of ash that ascended an estimated 30 km into the atmosphere. Glaze et al. (2011) assume a vent eruption velocity of 300 m/s, which was probably much higher than that of a typical Siberian Traps eruption based on mass-balance considerations. Under these conditions, convective plumes from linear vent geometries with fissures longer than 5 km approach the stability of plumes from circular vents. Over a wide range of vent widths, such plumes exceed 10 km in height.

Thus, while introduction of material to the stratosphere by traditional convective plumes was probably sporadic, episodes of higher mass-flux and explosivity during Siberian magmatism may have played an important role in delivering degassing volatiles to greater heights in the atmosphere.

5.4. Effects of S, Cl, and F injection into the atmosphere

The behavior of S in the atmosphere is better known than that of Cl or F. Volcanic SO_2 reacts with water to form sulfate aerosols, which increase the optical depth of the atmosphere (Devine et al., 1984; Robock, 2000; Sigurdsson, 1990; Sigurdsson et al., 1992; Wignall, 2001). The resultant global cooling may reach 3–4 K in the case of tropical super-eruptions such as the Younger Toba Tuff (Timmreck et al., 2010). Cooling related to sulfates in the stratosphere lasts on the order of 10 years, with maximum effects in the first 1–2 years (Robock, 2000; Timmreck et al., 2010; Wignall, 2001). On the other hand, flood basalt eruptions can sustain sulfur emissions over much longer periods than those associated with felsic super-eruptions, extending the radiative repercussions (Thordarson et al., 2009). High-latitude eruptions, unlike tropical eruptions, probably generate cooling that is restricted to the hemisphere of the eruption (Oman et al., 2005). The very high sulfate aerosol concentrations associated with super-eruptions may lead to faster removal from the atmosphere; at the same time, larger sulfate particles may form, limiting the potential increase in the optical depth of the atmosphere (Pinto et al., 1989; Timmreck et al., 2010).

Early assessments of Cl degassing concluded that volcanic Cl would be flushed from an ascending thermal plume due to dissolution in supercooled HCl–H_2O droplets and subsequent condensation and precipitation (Pinto et al., 1989; Tabazadeh and Turco, 1993). As a result of this co-condensation effect, water is one of the primary controls on HCl in volcanic plumes. If the mass ratio of HCl:H_2O in the plume increases significantly compared to the ratio of ~0.007 assumed in Pinto et al. (1989), it becomes more difficult to dissolve HCl. In this study, we document magmatic Cl:H_2O ratios that appear to exceed unity for some magmas.

The translation of our magmatic Cl:H_2O ratios into mixing ratios in the convective plume requires an assumption of degassing efficiencies and an estimate of the surface and atmospheric water that is entrained into the plume. For phreatomagmatic eruptions, the contribution of groundwater may be considerable. This water might help to flush out Cl. However, high-flux episodes of flood lava eruption that would more easily generate stratospheric plumes would entrain relatively less ambient air (Sparks et al., 1997; Woods, 1993), reducing the dilution of magmatic HCl. Our preliminary results and previous measurements of Noril'sk melt inclusions (Sobolev et al., 2009) suggest that Siberian Traps magmas were generally H_2O-poor, ranging from 0.03 to 0.94 wt.% H_2O.

In Fig. 6 we extend the vapor pressure curves of HCl in equilibrium with HCl–H_2O solutions as calculated by Nair et al. (1983) to higher HCl concentrations. HCl–H_2O aerosol droplets with 10 mass percent hydrochloric acid have HCl partial pressures significantly above the ambient stratospheric partial pressure of 2×10^{-8} Torr (Pinto et al., 1989), even at 215–220 K, the temperature of the high-latitude tropopause in winter (Gill, 1982; Randel and Wu, 2010). Consequently, with an assumption of equilibrium conditions some HCl would remain in the vapor phase and escape condensation. Because the stratosphere is very dry, any aqueous HCl that reaches it may also be subject to evaporation and a return to the gas phase (Pinto et al., 1989).

Thus, Fig. 6 suggests that in some cases the removal of Cl through the 'cold-trap' effect may be less efficient, and for a plume that

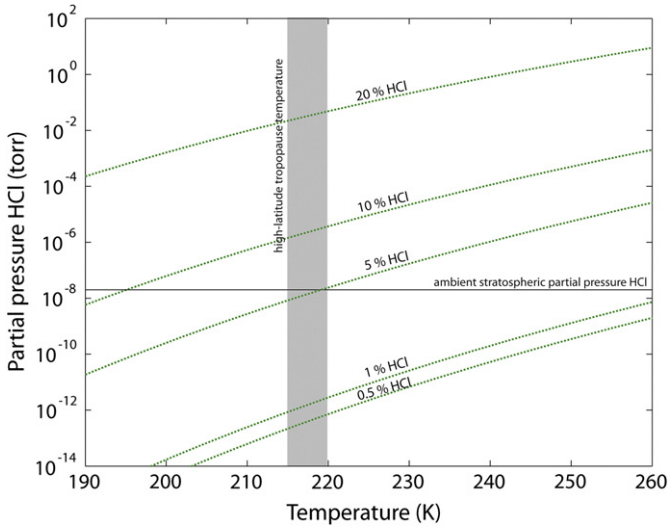

Fig. 6. Vapor pressure of HCl in equilibrium with HCl–H_2O solution aerosol of the HCl concentration noted on each curve. The gray vertical box shows the present-day temperature of the high-latitude tropopause (Gill, 1982; Randel and Wu, 2010). The solid horizontal line shows typical stratospheric partial pressure of HCl of 2×10^{-8} Torr (Pinto et al., 1989). Where HCl partial pressure curves exceed this threshold, HCl will not completely condense from the ascending plume.

penetrates the tropopause, significant Cl may then reach the stratosphere. This conclusion is consistent with aircraft measurements of the 2000 Hekla plume, which indicate that ~75% of volcanogenic Cl reached the stratosphere where it subsequently led to a reduction in observed ozone levels (Millard et al., 2006; Rose et al., 2006).

Cl can catalyze the destruction of ozone in the stratosphere through cycles that generally resemble:

$$Cl + O_3 \rightarrow ClO + O_2,$$
$$ClO + O \rightarrow Cl + O_2,$$
$$Net\ result: O_3 + O \rightarrow O_2 + O_2.$$

Beerling et al. (2007) estimate a total HCl release from the Siberian Traps of 2200 Gt based on Cl concentrations from the Columbia River Flood Basalts. They find that if released over 100 kyr, this quantity of HCl would result in between 26 and 55% ozone depletion. The release of HCl in pulses or in conjunction with generation of organohalogen precursors from heating of organic rich rocks would both result in additional ozone destruction.

Our estimate for the total degassing of Cl from the Siberian Traps is ~3400–8700 Gt, 1.5 to 4 times as large as the input used in the Beerling et al. (2007) model. 8700 Gt translates to 8.7×10^{18} g, seven orders of magnitude greater than the 5×10^{11} g Cl that is currently in the stratosphere (Pinto et al., 1989). Even if only a small fraction of volcanic Cl from the Siberian Traps was ultimately delivered to the stratosphere, possibly during pulses of particularly violent eruption, the effect on ozone levels could have been profound.

Fluorine and bromine may also be important chemical constituents of the erupted gas. The direct toxicity of F is well-known. For example, F from the Laki eruption was adsorbed onto tephra grains and resulted in fluorosis poisoning of Icelandic sheep (Thordarson and Self, 2003). While we have not directly measured Br concentrations, it behaves similarly to Cl, with a typical ratio of Cl/Br in the crust of ~273 (Bureau et al., 2000), and approximately 340–400 in the mantle (McDonough and Sun, 1995; Pyle and Mather, 2009). Bureau et al. (2000) use this ratio to estimate Br fluxes for eruptions with known Cl. By this method, we extrapolate to a tentative Br degassing from the Siberian Traps of the order of 10 Gt, or ~10^5 times the present-day stratospheric reservoir Br may oxidize in volcanic plumes, thereby reducing its solubility and avoiding the effects of co-condensation with water (Bureau et al., 2000). Br is also about two orders of magnitude more effective as a catalyst for the destruction of ozone than Cl (Daniel et al., 1999).

Because sulfate aerosols can also contribute to the activation of halogen compounds (Textor et al., 2003), future modeling of atmospheric chemistry and ozone depletion should investigate the combined effects of S, Cl, F, and Br based on our new constraints on volcanic emissions from the Siberian Traps.

6. Conclusions

We measure concentrations of S, Cl, and F in melt inclusions from the Siberian Traps. We estimate total magmatic degassing from the large igneous province of ~6300–7800 Gt sulfur, ~3400–8700 Gt chlorine, and ~7100–13,600 Gt fluorine. More robust constraints on degassing efficiencies, especially for intrusive rocks, would significantly improve the precision of degassing estimates. These fluxes would be in addition to any direct degassing from heating and contact metamorphism of rocks in the Tunguska sedimentary basin (Svensen et al., 2009). Early episodes of explosive volcanism could have increased the likelihood that volatiles would reach the stratosphere. High Cl concentrations may have allowed some fraction of degassing Cl to escape condensation in order to remain in the ascending plume.

The viability of the Siberian Traps as a trigger for the end-Permian extinction depends heavily on volatile emissions. In order to rigorously assess the effects of volcanic and metamorphic degassing from the Tunguska basin, further atmospheric chemistry and climate modeling is urgently needed. The high volatile contents which we report in this study for many Siberian Traps magmas, and in particular for massive dolerite sills, may have significantly contributed to wholesale deterioration of latest Permian and early Triassic ecosystems.

Supplementary materials related to this article can be found online at doi: 10.1016/j.epsl.2011.12.001.

Acknowledgments

This study was funded by grant EAR-0807585 from NSF Continental Dynamics, and supplemented by the MIT Wade Fund. The American Museum of Natural History graciously provided maymechite samples collected by Valeri Fedorenko. NSF grant EAR-0439888 supported the digital imaging lab, melt inclusion preparation supplies and salary of Ingrid Ukstins Peate. The gas-mixing furnace lab at University of Iowa was established through funds from National Science Foundation grant EAR-0609652 and University of Iowa start-up funds to Ingrid Ukstins Peate. Roman Veselovskiy, Vladimir Pavlov, and Seth Burgess were valued collaborators during field work. The authors gratefully thank Tim Grove, Nilanjan Chatterjee, Nobumichi Shimizu, Chien Wang, and Jay Thompson. Paul Wallace, Stephen Self, Thorvaldur Thordarson, and an anonymous reviewer provided thoughtful comments that greatly improved the quality of this manuscript.

References

Anderson, A.T., 1974. Chlorine, sulfur, and water in magmas and oceans. Geol. Soc. Am. Bull. 85, 1485–1492.
Ariskin, A.A., Frenkel, M.Y., Barmina, G.S., Nielsen, R.L., 1993. COMAGMAT — a Fortran program to model magma differentiation processes. Comput. Geosci. 19, 1155–1170.
Arndt, N.T., Christensen, U., 1992. The role of lithospheric mantle in continental flood volcanism — thermal and geochemical constraints. J. Geophys. Res. Solid Earth 97, 10967–10981.
Arndt, N., Lehnert, K., Vasilev, Y., 1995. Meimechites — highly magnesian lithosphere-contaminated alkaline magmas from deep subcontinental mantle. Lithos 34, 41–59.
Arndt, N., Chauvel, C., Czamanske, G., Fedorenko, V., 1998. Two mantle sources, two plumbing systems: tholeiitic and alkaline magmatism of the Maymecha River Basin, Siberian flood volcanic province. Contrib. Mineral. Petrol. 133, 297–313.
Barnes, J.E., Hofmann, D.J., 1997. Lidar measurements of stratospheric aerosol over Mauna Loa Observatory. Geophys. Res. Lett. 24, 1923–1926.

Beerling, D.J., Harfoot, M., Lomax, B., Pyle, J.A., 2007. The stability of the stratospheric ozone layer during the end-Permian eruption of the Siberian Traps. Philos. Trans. R Soc. Lond. A 365, 1843–1866.
Blake, S., Self, S., Sharma, K., Sephton, S., 2010. Sulfur release from the Columbia River Basalts and other flood lava eruptions constrained by a model of sulfide saturation. Earth Planet. Sci. Lett. 299, 328–338.
Bowring, S.A., Erwin, D.H., Jin, Y.G., Martin, M.W., Davidek, K., Wang, W., 1998. U/Pb zircon geochronology and tempo of the end-Permian mass extinction. Science 280, 1039–1045.
Bryan, S.E., Peate, I.U., Peate, D.W., Self, S., Jerram, D.A., Mawby, M.R., Marsh, J.S., Miller, J.A., 2010. The largest volcanic eruptions on Earth. Earth Sci. Rev. 102, 207–229.
Bureau, H., Keppler, H., Metrich, N., 2000. Volcanic degassing of bromine and iodine: experimental fluid/melt partitioning data and applications to stratospheric chemistry. Earth Planet. Sci. Lett. 183, 51–60.
Caldeira, K., Rampino, M.R., 1990. Carbon-dioxide emissions from Deccan volcanism and a K/T boundary greenhouse-effect. Geophys. Res. Lett. 17, 1299–1302.
Campbell, I.H., Czamanske, G.K., Fedorenko, V.A., Hill, R.I., Stepanov, V., 1992. Synchronism of the Siberian Traps and the Permian–Triassic boundary. Science 258, 1760–1763.
Cao, C.Q., Love, G.D., Hays, L.E., Wang, W., Shen, S.Z., Summons, R.E., 2009. Biogeochemical evidence for euxinic oceans and ecological disturbance presaging the end-Permian mass extinction event. Earth Planet. Sci. Lett. 281, 188–201.
Carroll, M.R., Webster, J.D., 1994. Solubilities of Sulfur, Noble-Gases, Nitrogen, Chlorine, and Fluorine in Magmas, Volatiles in Magmas, pp. 231–279.
Cocks, L.R.M., Torsvik, T.H., 2007. Siberia, the wandering northern terrane, and its changing geography through the Palaeozoic. Earth Sci. Rev. 82, 29–74.
Coffin, M., Eldholm, O., 1994. Large igneous provinces: crustal structure, dimensions, and external consequences. Rev. Geophys. 32, 1–36.
Cottrell, E., Spiegelman, M., Langmuir, C.H., 2002. Consequences of diffusive reequilibration for the interpretation of melt inclusions. Geochem. Geophys. Geosyst. 3.
Dalrymple, G.B., Czamanske, G.K., Fedorenko, V.A., Simonov, O.N., Lanphere, M.A., Likhachev, A.P., 1995. A reconnaissance Ar-40/Ar-39 geochronological study of ore-bearing and related rocks, Siberian Russia. Geochim. Cosmochim. Acta 59, 2071–2083.
Daniel, J.S., Solomon, S., Portmann, R.W., Garcia, R.R., 1999. Stratospheric ozone destruction: the importance of bromine relative to chlorine. J. Geophys. Res.-Atmos. 104, 23871–23880.
Danyushevsky, L.V., Della-Pasqua, F.N., Sokolov, S., 2000. Re-equilibration of melt inclusions trapped by magnesian olivine phenocrysts from subduction-related magmas: petrological implications. Contrib. Mineral. Petrol. 138, 68–83.
Danyushevsky, L.V., Sokolov, S., Falloon, T.J., 2002. Melt inclusions in olivine phenocrysts: using diffusive re-equilibration to determine the cooling history of a crystal, with implications for the origin of olivine-phyric volcanic rocks. J. Petrol. 43, 1651–1671.
Devine, J.D., Sigurdsson, H., Davis, A.N., Self, S., 1984. Estimates of sulfur and chlorine yield to the atmosphere from volcanic-eruptions and potential climatic effects. J. Geophys. Res. 89, 6309–6325.
Edmonds, M., Gerlach, T.M., Herd, R.A., 2009. Halogen degassing during ascent and eruption of water-poor basaltic magma. Chem. Geol. 263, 122–130.
Erwin, D.H., 1994. The Permo-Triassic extinction. Nature 367, 231–236.
Farley, K.A., Ward, P., Garrison, G., Mukhopadhyay, S., 2005. Absence of extraterrestrial He-3 in Permian–Triassic age sedimentary rocks. Earth Planet. Sci. Lett. 240, 265–275.
Fedorenko, V.A., Czamanske, G.K., 1997. Results of new field and geochemical studies of the volcanic and intrusive rocks of the Maymecha–Kotuy area, Siberian Flood-Basalt Province, Russia. Int. Geol. Rev. 39, 479–531.
Fedorenko, V.A., Lightfoot, P.C., Czamanske, G.K., Hawkesworth, C.J., Wooden, J.L., Ebel, D.S., 1996. Petrogenesis of the Siberian Flood-Basalt Sequence at Noril'sk. Int. Geol. Rev. 38, 99–135.
Fedorenko, V., Czamanske, G., Zen'ko, T., Budahn, J., Siems, D., 2000. Field and geochemical studies of the melilite-rearing Arydzhangsky suite, and an overall perspective on the Siberian alkaline-ultramafic flood-volcanic rocks. Int. Geol. Rev. 42, 769–804.
Ganino, C., Arndt, N.T., 2009. Climate changes caused by degassing of sediments during the emplacement of large igneous provinces. Geology 37, 323–326.
Gerlach, T.M., Graeber, E.J., 1985. Volatile budget of Kilauea volcano. Nature 313, 273–277.
Gilbert, J.S., Lane, S.J., 1994. The origin of accretionary lapilli. Bull. Volcanol. 56, 398–411.
Gill, A.E., 1982. Atmosphere–Ocean Dynamics.
Glaze, L.S., Baloga, S.M., Wimert, J., 2011. Explosive volcanic eruptions from linear vents on Earth, Venus, and Mars: comparisons with circular vent eruptions. J. Geophys. Res. 116, E01011.
Grise, K.M., Thompson, D.W.J., Birner, T., 2010. A global survey of static stability in the stratosphere and upper troposphere. J. Clim. 23, 2275–2292.
Hauri, E., 2002. Sims analysis of volatiles in silicate glasses, 2: isotopes and abundances in Hawaiian melt inclusions. Chem. Geol. 183, 115–141.
Hawkesworth, C.J., Lightfoot, P.C., Fedorenko, V.A., Blake, S., Naldrett, A.J., Doherty, W., Gorbachev, N.S., 1995. Magma differentiation and mineralization in the Siberian continental flood basalts. Lithos 34, 61–88.
Huey, R.B., Ward, P.D., 2005. Hypoxia, global warming, and terrestrial Late Permian extinctions. Science 308, 398–401.
Isozaki, Y., 1997. Permo-Triassic boundary superanoxia and stratified superocean: records from lost deep sea. Science 276, 235–238.
Jay, A.E., Widdowson, M., 2008. Stratigraphy, structure and volcanology of the Se Deccan continental flood basalt province: implications for eruptive extent and volumes. J. Geol. Soc. 165, 177–188.
Johnston, D.A., 1980. Volcanic contribution of chlorine to the stratosphere — more significant to ozone than previously estimated. Science 209, 491–493.
Kamo, S.L., Czamanske, G.K., Amelin, Y., Fedorenko, V.A., Davis, D.W., Trofimov, V.R., 2003. Rapid eruption of Siberian flood-volcanic rocks and evidence for coincidence with the Permian–Triassic boundary and mass extinction at 251 Ma. Earth Planet. Sci. Lett. 214, 75–91.
Kent, A.J.R., Clague, D.A., Honda, M., Stolper, E.M., Hutcheon, I.D., Norman, M.D., 1999a. Widespread assimilation of a seawater-derived component at Loihi Seamount, Hawaii. Geochim. Cosmochim. Acta 63, 2749–2761.
Kent, A.J.R., Norman, M.D., Hutcheon, I.D., Stolper, E.M., 1999b. Assimilation of seawater-derived components in an oceanic volcano: evidence from matrix glasses and glass inclusions from Loihi Seamount, Hawaii. Chem. Geol. 156, 299–319.
Keszthelyi, L., Self, S., Thordarson, T., 2006. Flood lavas on Earth, Io and Mars. J. Geol. Soc. 163, 253–264.
Knoll, A.H., Barnbach, R.K., Payne, J.L., Pruss, S., Fischer, W.W., 2007. Paleophysiology and end-Permian mass extinction. Earth Planet. Sci. Lett. 256, 295–313.
Kontorovich, A.E., Khomenko, A.V., Burshtein, L.M., Likhanov, I.I., Pavlov, A.L., Staroseltsev, V.S., Ten, A.A., 1997. Intense basic magmatism in the Tunguska Petroleum Basin, Eastern Siberia, Russia. Pet. Geosci. 3, 359–369.
Kump, L.R., Pavlov, A., Arthur, M.A., 2005. Massive release of hydrogen sulfide to the surface ocean and atmosphere during intervals of oceanic anoxia. Geology 33, 397–400.
Lehrmann, D.J., Ramezani, J., Bowring, S.A., Martin, M.W., Montgomery, P., Enos, P., Payne, J.L., Orchard, M.J., Wang, H.M., Wei, J.Y., 2006. Timing of recovery from the end-Permian extinction: geochronologic and biostratigraphic constraints from South China. Geology 34, 1053–1056.
Li, C., Ripley, E.M., Naldrett, A.J., Schmitt, A.K., Moore, C.H., 2009a. Magmatic anhydrite-sulfide assemblages in the plumbing system of the Siberian Traps. Geology 37, 259–262.
Li, C.S., Ripley, E.M., Naldrett, A.J., 2009b. A new genetic model for the giant Ni–Cu-Pge sulfide deposits associated with the Siberian Flood Basalts. Econ. Geol. 104, 291–301.
Lightfoot, P.C., Naldrett, A.J., Gorbachev, N.S., Doherty, W., Fedorenko, V.A., 1990. Geochemistry of the Siberian Trap of the Norilsk Area, Ussr, with implications for the relative contributions of crust and mantle to flood-basalt magmatism. Contrib. Mineral. Petrol. 104, 631–644.
Malitch, N.S., Mironyuk, E.P., Tuganova, E.V., 1999. Geological Map of Siberian Platform and Adjoining Areas. Ministry of Natural Resources of the Russian Federation.
Mavrogenes, J.A., O'Neill, H.S.C., 1999. The relative effects of pressure, temperature and oxygen fugacity on the solubility of sulfide in mafic magmas. Geochim. Cosmochim. Acta 63, 1173–1180.
McDonough, W.F., Sun, S.S., 1995. The composition of the Earth. Chem. Geol. 120, 223–253.
Metrich, N., Wallace, P.J., 2008. Volatile abundances in basaltic magmas and their degassing paths tracked by melt inclusions. In: Putirka, K.D., Tepley, F.J. (Eds.), Minerals, Inclusions and Volcanic Processes, pp. 363–402.
Meyerhoff, A.A., 1980. Geology and petroleum fields in Proterozoic and Lower Cambrian Strata, Lena-Tunguska Petroleum Province, Eastern Siberia, Ussr. In: Halbouty, M.T. (Ed.), Giant Oil and Gas Fields of the Decade 1968–1978. American Association of Petroleum Geologists.
Michael, P.J., Cornell, W.C., 1998. Influence of spreading rate and magma supply on crystallization and assimilation beneath mid-ocean ridges: evidence from chlorine and major element chemistry of Mid-Ocean Ridge Basalts. J. Geophys. Res. Solid Earth 103, 18325–18356.
Michael, P.J., Schilling, J.G., 1989. Chlorine in Mid-Ocean Ridge Magmas: evidence for assimilation of seawater-influenced components. Geochim. Cosmochim. Acta 53, 3131–3143.
Millard, G.A., Mather, T.A., Pyle, D.M., Rose, W.I., Thornton, B., 2006. Halogen emissions from a small volcanic eruption: modeling the peak concentrations, dispersion, and volcanically induced ozone loss in the stratosphere. Geophys. Res. Lett. 33.
Molina, M.J., 1996. Role of chlorine in stratospheric chemistry. Pure Appl. Chem. 68, 1749–1756.
Nair, P.V.N., Joshi, P.V., Mishra, U.C., Vohra, K.G., 1983. Growth of aqueous-solution droplets of HNO_3 and HCl in the atmosphere. J. Atmos. Sci. 40, 107–115.
Naldrett, A.J., Lightfoot, P.C., Fedorenko, V., Doherty, W., Gorbachev, N.S., 1992. Geology and geochemistry of intrusions and flood basalts of the Norilsk Region, Ussr, with implications for the origin of the Ni–Cu ores. Econ. Geol. Bull. Soc. Econ. Geol. 87, 975–1004.
Naumov, V.A., Ankudimova, L.A., 1995. Palynological complexes and age of volcanic sediments of the Angara–Katanga District, Middle Angara Region. Geol. Geophys. 36.
Newman, S., Lowenstern, J.B., 2002. VolatileCalc: a silicate melt–H_2O–CO_2 solution model written in visual basic for Excel. Comput. Geosci. 28, 597–604.
Oman, L., Robock, A., Stenchikov, G., Schmidt, G.A., Ruedy, R., 2005. Climatic response to high-latitude volcanic eruptions. J. Geophys. Res.-Atmos. 110.
Pavlov, V.E., Fluteau, F., Veselovskiy, R.V., Fetisova, A.M., Latyshev, A.V., 2011. Secular geomagnetic variations and volcanic pulses in the Permian–Triassic Traps of the Norilsk and Maimecha–Kotui Provinces. Izv. Phys. Solid Earth 47, 402–417.
Payne, J.L., Kump, L.R., 2007. Evidence for recurrent early Triassic massive volcanism from quantitative interpretation of carbon isotope fluctuations. Earth Planet. Sci. Lett. 256, 264–277.
Payne, J.L., Lehrmann, D.J., Wei, J.Y., Orchard, M.J., Schrag, D.P., Knoll, A.H., 2004. Large perturbations of the carbon cycle during recovery from the end-Permian extinction. Science 305, 506–509.
Pinto, J.P., Turco, R.P., Toon, O.B., 1989. Self-limiting physical and chemical effects in volcanic-eruption clouds. J. Geophys. Res.-Atmos. 94, 11165–11174.
Putirka, K., 1999. Clinopyroxene plus liquid equilibria to 100 kbar and 2450 K. Contrib. Mineral. Petrol. 135, 151–163.
Pyle, D.M., Mather, T.A., 2009. Halogens in igneous processes and their fluxes to the atmosphere and oceans from volcanic activity: a review. Chem. Geol. 263, 110–121.
Qin, Z.W., Lu, F.Q., Anderson, A.T., 1992. Diffusive reequilibration of melt and fluid inclusions. Am. Mineral. 77, 565–576.

Randel, W.J., Wu, F., 2010. The polar summer tropopause inversion layer. J. Atmos. Sci. 67, 2572–2581.
Reichow, M.K., Saunders, A.D., White, R.V., Al'Mukhamedov, A.L., Medvedev, A.Y., 2005. Geochemistry and petrogenesis of basalts from the West Siberian Basin: an extension of the Permo-Triassic Siberian Traps, Russia. Lithos 79, 425–452.
Reichow, M.K., Pringle, M.S., Al'Mukhamedov, A.I., Allen, M.B., Andreichev, V.L., Buslov, M.M., Davies, C.E., Fedoseev, G.S., Fitton, J.G., Inger, S., Medvedev, A.Y., Mitchell, C., Puchkov, V.N., Safonova, I.Y., Scott, R.A., Saunders, A.D., 2009. The timing and extent of the eruption of the Siberian Traps large igneous province: implications for the end-Permian environmental crisis. Earth Planet. Sci. Lett. 277, 9–20.
Renne, P.R., Basu, A.R., 1991. Rapid eruption of the Siberian Traps flood basalts at the Permo-Triassic boundary. Science 253, 176–179.
Renne, P.R., Zhang, Z.C., Richards, M.A., Black, M.T., Basu, A.R., 1995. Synchrony and causal relations between Permian–Triassic boundary crises and Siberian flood volcanism. Science 269, 1413–1416.
Ripley, E.M., Lightfoot, P.C., Li, C., Elswick, E.R., 2003. Sulfur isotopic studies of continental flood basalts in the Noril'sk region: implications for the association between lavas and ore-bearing intrusions. Geochim. Cosmochim. Acta 67, 2805–2817.
Robock, A., 2000. Volcanic eruptions and climate. Rev. Geophys. 38, 191–219.
Rose, W.I., Millard, G.A., Mather, T.A., Hunton, D.E., Anderson, B., Oppenheimer, C., Thornton, B.F., Gerlach, T.M., Viggiano, A.A., Kondo, Y., Miller, T.M., Ballenthin, J.O., 2006. Atmospheric chemistry of a 33–34 hour old volcanic cloud from Hekla Volcano (Iceland): insights from direct sampling and the application of chemical box modeling. J. Geophys. Res.-Atmos. 111.
Ross, P.S., Peate, I.U., McClintock, M.K., Xu, Y.G., Skilling, I.P., White, J.D.L., Houghton, B.F., 2005. Mafic volcaniclastic deposits in flood basalt provinces: a review. J. Volcanol. Geotherm. Res. 145, 281–314.
Rowe, M.C., Lassiter, J.C., 2009. Chlorine enrichment in Central Rio Grande Rift basaltic melt inclusions: evidence for subduction modification of the lithospheric mantle. Geology 37, 439–442.
Ryabov, V.V., Konenko, V.F., Khmelnikova, O.S., 1985. Rock-forming minerals of picritic basalts of the norilsk region. Sov. Geol. Geophys. 26, 77–84.
Saal, A.E., Hauri, E.H., Langmuir, C.H., Perfit, M.R., 2002. Vapour undersaturation in primitive Mid-Ocean-Ridge Basalt and the volatile content of Earth's upper mantle. Nature 419, 451–455.
Schilling, J.G., Bergeron, M.B., Evans, R., 1980. Halogens in the mantle beneath the North-Atlantic. Philos. Trans. R Soc. Lond. A Math. Phys. Eng. Sci. 297, 147–178.
Schumacher, R., Schmincke, H.U., 1995. Models for the origin of accretionary lapilli. Bull. Volcanol. 56, 626–639.
Self, S., Thordarson, T., Keszthelyi, L., Walker, G.P.L., Hon, K., Murphy, M.T., Long, P., Finnemore, S., 1996. A new model for the emplacement of Columbia River basalts as large, inflated pahoehoe lava flow fields. Geophys. Res. Lett. 23, 2689–2692.
Self, S., Blake, S., Sharma, K., Widdowson, M., Sephton, S., 2008. Sulfur and chlorine in late cretaceous Deccan magmas and eruptive gas release. Science 319, 1654–1657.
Sepkoski, J.J., Bambach, R.K., Raup, D.M., Valentine, J.W., 1981. Phanerozoic marine diversity and the fossil record. Nature 293, 435–437.
Sharma, M., Basu, A.R., Nesterenko, G.V., 1991. Nd–Sr isotopes, petrochemistry, and origin of the Siberian Flood Basalts, Ussr. Geochim. Cosmochim. Acta 55, 1183–1192.
Sigurdsson, H., 1990. Evidence of volcanic loading of the atmosphere and climate response. Glob. Planet. Chang. 89, 277–289.
Sigurdsson, H., Dhondt, S., Carey, S., 1992. The impact of the Cretaceous Tertiary bolide on evaporite terrane and generation of major sulfuric-acid aerosol. Earth Planet. Sci. Lett. 109, 543–559.
Sisson, T.W., Grove, T.L., 1993. Experimental investigations of the role of H_2O in calc-alkaline differentiation and subduction zone magmatism. Contrib. Mineral. Petrol. 113, 143–166.
Sobolev, A.V., Kamenetsky, V.S., Kononkova, N.N., 1991. New data on petrology of Siberia meymechites. Geokhimiya 1084–1095.
Sobolev, A., Krivolutskaya, N., Kuzmin, D., 2009. Petrology of the parental melts and mantle sources of Siberian Trap magmatism. Petrology 17, 253–286.
Sobolev, S.V., Sobolev, A.V., Kuzmin, D.V., Krivolutskaya, N.A., Petrunin, A.G., Arndt, N.T., Radko, V.A., Vasiliev, Y.R., 2011. Linking mantle plumes, large igneous provinces and environmental catastrophes. Nature 477, 312–U380.
Sparks, R.S.J., Bursik, M.I., Carey, S.N., Gilbert, J.S., Glaze, L.S., Sigurdsson, H., Woods, A.W., 1997. Volcanic Plumes. Wiley and Sons, Chichester, England.
Stothers, R.B., Wolff, J.A., Self, S., Rampino, M.R., 1986. Basaltic fissure eruptions, plume heights, and atmospheric aerosols. Geophys. Res. Lett. 13, 725–728.
Svensen, H., Planke, S., Polozov, A.G., Schmidbauer, N., Corfu, F., Podladchikov, Y.Y., Jamtveit, B., 2009. Siberian gas venting and the end-Permian environmental crisis. Earth Planet. Sci. Lett. 277, 490–500.
Tabazadeh, A., Turco, R.P., 1993. Stratospheric chlorine injection by volcanic-eruptions — HCl scavenging and implications for ozone. Science 260, 1082–1086.
Textor, C., Graf, H.F., Herzog, M., Oberhuber, J.M., 2003. Injection of gases into the stratosphere by explosive volcanic eruptions. J. Geophys. Res.-Atmos. 108.
Thordarson, T., Self, S., 1993. The Laki (Skaftar-Fires) and Grimsvotn eruptions in 1783–1785. Bull. Volcanol. 55, 233–263.
Thordarson, T., Self, S., 1996. Sulfur, chlorine and fluorine degassing and atmospheric loading by the Roza Eruption, Columbia River Basalt Group, Washington, USA. J. Volcanol. Geotherm. Res. 74, 49–73.
Thordarson, T., Self, S., 1998. The Roza Member, Columbia River Basalt Group: a gigantic pahoehoe lava flow field formed by endogenous processes? J. Geophys. Res. Solid Earth 103, 27411–27445.
Thordarson, T., Self, S., 2003. Atmospheric and environmental effects of the 1783–1784 Laki eruption: a review and reassessment. J. Geophys. Res.-Atmos. 108.
Thordarson, T., Self, S., Oskarsson, N., Hulsebosch, T., 1996. Sulfur, chlorine, and fluorine degassing and atmospheric loading by the 1783–1784 Ad Laki (Skaftar Fires) eruption in Iceland. Bull. Volcanol. 58, 205–225.
Thordarson, T., Rampino, M., Keszthelyi, L., Self, S., 2009. Effects of megascale eruptions on Earth and Mars. In: Chapman, M.G., Keszthelyi, L. (Eds.), Preservation of Random Megascale Events on Mars and Earth: Influence on Geologic History: Geol Soc Am Spec Paper, pp. 37–53.
Timmreck, C., Graf, H.F., Lorenz, S.J., Niemeier, U., Zanchettin, D., Matei, D., Jungclaus, J.H., Crowley, T.J., 2010. Aerosol size confines climate response to volcanic super-eruptions. Geophys. Res. Lett. 37.
Vasil'ev, Y.R., Zolotukhin, V.V., Feoktistov, G.D., Prusskaya, S.N., 2000. Evaluation of the volumes and genesis of Permo-Triassic trap magmatism on the Siberian Platform. Geol. Geofiz. 41, 1696–1705.
Visscher, H., Looy, C.V., Collinson, M.E., Brinkhuis, H., Cittert, J., Kurschner, W.M., Sephton, M.A., 2004. Environmental mutagenesis during the end-Permian ecological crisis. Proc. Natl. Acad. Sci. U. S. A. 101, 12952–12956.
Walker, G.P.L., Self, S., Wilson, L., 1984. Tarawera 1886, New Zealand — a basaltic plinian fissure eruption. J. Volcanol. Geotherm. Res. 21, 61–78.
Wallace, P., Carmichael, I.S.E., 1992. Sulfur in basaltic magmas. Geochim. Cosmochim. Acta 56, 1863–1874.
Webster, J.D., Kinzler, R.J., Mathez, E.A., 1999. Chloride and water solubility in basalt and andesite melts and implications for magmatic degassing. Geochim. Cosmochim. Acta 63, 729–738.
Wei, L.J., Mosley-Thompson, E., Gabrielli, P., Thompson, L.G., Barbante, C., 2008. Synchronous deposition of volcanic ash and sulfate aerosols over Greenland in 1783 from the Laki eruption (Iceland). Geophys. Res. Lett. 35.
Wignall, P.B., 2001. Large igneous provinces and mass extinctions. Earth Sci. Rev. 53, 1–33.
Wooden, J.L., Czamanske, G.K., Fedorenko, V.A., Arndt, N.T., Chauvel, C., Bouse, R.M., King, B.S.W., Knight, R.J., Siems, D.F., 1993. Isotopic and trace-element constraints on mantle and crustal contributions to Siberian Continental Flood Basalts, Norilsk Area, Siberia. Geochim. Cosmochim. Acta 57, 3677–3704.
Woods, A.W., 1993. Moist convection and the injection of volcanic ash into the atmosphere. J. Geophys. Res. Solid Earth 98, 17627–17636.
Zharkov, M.A., 1984. Paleozoic Salt Bearing Formations of the World. Springer-Verlag, Berlin.
Zolotukhin, V.V., Almukhamedov, A.I., 1988. Traps of the Siberian Platform. In: Macdougall, J.D. (Ed.), Continental Flood Basalts. Kluwer Academic Publishers, Dordrecht.